Electron spin echo of $Cu^{2+}$ in the triglycine sulfate crystal family (TGS, TGSe, TGFB): electron spin–lattice relaxation, Debye temperature and spin–phonon coupling



2006 J. Phys.: Condens. Matter 18 6159

(http://iopscience.iop.org/0953-8984/18/26/033)

INSTITUTE OF PHYSICS PUBLISHING JOURNAL OF PHYSICS: CONDENSED MATTER

J. Phys.: Condens. Matter **18** (2006) 6159–6169 doi:10.1088/0953-8984/18/26/033

# Electron spin echo of $Cu^{2+}$ in the triglycine sulfate crystal family (TGS, TGSe, TGFB): electron spin–lattice relaxation, Debye temperature and spin–phonon coupling

**S Lijewski, J Goslar and S K Hoffmann**[1]

Institute of Molecular Physics, Polish Academy of Sciences, Smoluchowskiego 17, Pl-60 179 Poznan, Poland

E-mail: skh@ifmpan.poznan.pl

Received 3 April 2006, in final form 30 May 2006
Published 19 June 2006
Online at stacks.iop.org/JPhysCM/18/6159

**Abstract**

The electron spin–lattice relaxation of $Cu^{2+}$ has been studied by the electron spin echo technique in the temperature range 4.2–115 K in triglycine sulfate (TGS) family crystals. Assuming that the relaxation is due to Raman relaxation processes the Debye temperature $\Theta_D$ was determined as 190 K for TGS, 168 K for triglycine selenate (TGSe) and 179 K for triglycine fluoroberyllate (TGFB). We also calculated the $\Theta_D$ values from the sound velocities derived from available elastic constants. The elastic Debye temperatures were found as 348 K for TGS, 288 K for TGSe and 372 K for TGFB. The results shown good agreement with specific heat data for TGS. The elastic $\Theta_D$ are considerably larger than those determined from the Raman spin–lattice relaxation. The possible reasons for this discrepancy are discussed. We propose to use a modified expression describing two-phonon Raman relaxation with a single variable only ($\Theta_D$) after elimination of the sound velocity. Moreover, we show that the relaxation data can be fitted using the elastic Debye temperature value as a constant with an additional relaxation process contributing at low temperatures. This mechanism can be related to a local mode of the $Cu^{2+}$ defect in the host lattice. Electron paramagnetic resonance $g$-factors and hyperfine splitting were analysed in terms of the molecular orbital theory and the d-orbital energies and covalency factors of the $Cu(gly)_2$ complexes were found. Using the structural data and calculated orbital energies the spin–phonon coupling matrix element of the second-order Raman process was calculated as 553 $cm^{-1}$ for TGS, 742 $cm^{-1}$ for TGSe and 569 $cm^{-1}$ for TGFB.

[1] Author to whom any correspondence should be addressed.

  

## 1. Introduction

Triglycine family crystals $(NH_2CH_2COOH)_3{\cdot}H_2AX_4$ ($AX_4 = SO_4, SeO_4, BeF_4$) abbreviated as TGS, TGSe and TGFB, respectively, are well known monoclinic (see table 1 for unit cell parameters) isostructural ferroelectric materials with ordering temperatures above room temperature [1]. Paramagnetic ions of the iron group, such as $Cu^{2+}$, $Cr^{3+}$ and $VO^{2+}$, introduced to the host lattice are located in an interstitial positions and coordinated by two glycine ions in *trans* position and by two X-atoms at the apical positions (figure 1(a)). Continuous wave (cw) electron paramagnetic resonance (EPR) data are available for all three crystals [2], but we have only performed pulsed EPR studies previously for $Cu^{2+}$ ions in TGSe [3]. The results have shown that spins of $Cu^{2+}$ ions are well coupled to the lattice and that the electron spin–lattice relaxation is dominated by two-phonon Raman processes with a strongly temperature dependent relaxation rate $1/T_1$:

$$\frac{1}{T_1} = c \cdot T^9 \cdot I_8(\Theta_D/T) \tag{1}$$

where $c$ is a coefficient depending on the relaxation mechanism and $I_8$ is the transport integral over a Debye-type phonon spectrum having the Debye temperature $\Theta_D$. The $c$-coefficient and Debye temperature are two fitting parameters to experimental $1/T_1$ data. In this paper we look closely at both parameters in isostructural crystals of the TGS family and discuss their relation to the crystal structure and lattice dynamics. We present results of electron spin echo (ESE) measurements of the spin–lattice relaxation of $Cu^{2+}$ in TGS and TGFB single crystals and we compare these with results for $Cu^{2+}$ in TGSe [3].

Two problems are discussed in this paper. The first is related to the Debye $\Theta_D$ temperature value. Most of the available $\Theta_D$ data are for ionic or covalent crystals from specific heat measurements at very low temperatures ($T < 0.01\Theta_D$). Such a $\Theta_D$ is called the 'calorimetric' Debye temperature. Generally, the calorimetric $\Theta_D$ agrees well with the 'elastic' $\Theta_D$ calculated from sound velocity determined at a single temperature (mostly room temperature). Our 'Raman-relaxation' $\Theta_D$ is determined from a computer fitting to the spin relaxation experimental data collected in relatively broad temperature range (usually 4–60 K) where the density of phonon states is expected to follow $\omega^2$ dependence predicted by the Debye model. A problem is that the Raman-relaxation Debye temperature differs (it is considerably lower than) from calorimetric and elastic $\Theta_D$ values. In this paper we discuss possible sources of this discrepancy.

The second problem is related to the spin–phonon (orbit–lattice) coupling which is the mechanism of the spin–lattice relaxation and determines the probability of transition between spin levels. This coupling can only be very roughly estimated theoretically in terms of the crystal field theory [4] and no progress has been observed on this point since the 1960s. For this reason our idea is to collect experimental values of the coupling parameter which can suggest possible improvements to the existing old theories. The electron–phonon coupling has been evaluated for rare earth ions in some ionic crystals as being of the order of tens of $cm^{-1}$ [5]. One can expect that the coupling coefficient will be larger for iron group transition ions, but it has been only roughly estimated for some ions like $Mn^{2+}$ [6]. The spin–phonon coupling can be calculated from the experimental parameter $c$ of the equation (1) when crystallographic data, sound velocity and orbital splitting are available. We have calculated the sound velocity from published elastic constants, and we have calculated orbital energies from available EPR parameters ($g$-factors and hyperfine splitting).

**Table 1.** Structure of triglycine family crystals and EPR parameters and Raman relaxation parameters of $Cu^{2+}$ ions doped to the crystals.

| | TGS | TGSe | TGFB |
|---|---|---|---|
| Unit cell parameters[a] | | | |
| $a, b, c$ (Å), $\beta$ (deg) | 9.42, 12.64, 5.73, 110° | 9.54, 12.92, 5.86, 110° | 9.59, 12.75, 5.70, 112° |
| $V_u$ ($m^3$), $\rho$ (g $cm^{-3}$) | $0.6403 \times 10^{-27}$, 1.677 | $0.6787 \times 10^{-27}$, 1.811 | $0.6462 \times 10^{-27}$, 1.604 |
| $Cu^{2+}$ concentration (ions $cm^{-3}$) | $1.5 \times 10^{18}$ | $8 \times 10^{17}$ | $3 \times 10^{17}$ |
| EPR $Cu^{2+}$ parameters[b] | | | |
| $g_z, g_y, g_x$ | 2.261, 2.064, 2.054 | 2.260, 2.065, 2.053 | 2.24, 2.06, 2.06 |
| $A_z, A_y, A_x$ ($10^{-4}$ $cm^{-1}$) | $-150.1, \pm 5.0, \mp 30.0$ | $-151.0, 2.5, -42.2$ | $-132, 10, -32$ |
| Covalence factors $\alpha^2, \beta_1^2$ | 0.71(1), 0.92(3) | 0.69(1), 0.95(3) | 0.70(1), 0.75(3) |
| Fermi constant $\kappa$ | 0.40(1) | 0.42(1) | 0.39(1) |
| Orbital energy ($cm^{-1}$) $xy, xz, yz$ ($\pm 150$) | 17 000, 19 000, 22 600 | 17 100, 18 200, 22 400 | 14 700, 20 000 |

| $T_1$ relaxation data | | | | | | |
|---|---|---|---|---|---|---|
| | Raman | Fit ($\Theta_D$-elastic) | Raman | Fit ($\Theta_D$-elastic) | Raman | Fit ($\Theta_D$-elastic) |
| Coefficient $b$ ($K^{-1}$ $s^{-1}$) | 96 | 0 | 204.2 | 0 | 435.2 | 390 |
| Raman coefficient $c$ ($K^{-9}$ $s^{-1}$) | $7 \times 10^{-14}$ | $6 \times 10^{10}$ | $7.5 \times 10^{-13}$ | $9 \times 10^{10}$ | $1 \times 10^{-13}$ | $8 \times 10^{10}$ |
| Optical phonon | | | | | | |
| Coefficient $f$ ($s^{-1}$) | $2.03 \times 10^8$ | $1.03 \times 10^8$ | — | 0 | — | 0 |
| Mode energy ($cm^{-1}$) | 486 | 485 | — | 0 | — | 0 |

[a] Data from [29–31].
[b] $g$ and $A$ parameters from [21–24].

## 2. Experimental details

Large high quality single crystals of triglycine sulfate ($(NH_2CH_2COOH)_3 \cdot H_2SO_4 \equiv$ TGS) and triglycine fluoroberyllate ($(NH_2CH_2COOH)_3 \cdot H_2BeF_4 \equiv$ TGFB) were grown by slow evaporation from a saturated aqueous solution containing equimolar amounts of glycine and sulfuric or fluoroberyllic acid with a few per cent of $CuSO_4 \cdot 5H_2O$.

The number of admixture $Cu^{2+}$ ions in crystals was determined from the EPR spectral intensity as about $10^{17}$–$10^{18}$ ions $cm^{-3}$ (see table 1).

Experiments were performed on a Bruker ESP 380E FT/CW spectrometer equipped with an Oxford CF935 flowing helium cryostat. EPR spectra were well resolved and the pulsed EPR experiments were performed along the $z$-axis of the $g$-tensor (marked in figure 1(a)) for selected hyperfine line ($m_I = -1/2$) as marked by the asterisk in the spectrum presented in figure 1(b). The spin-Hamiltonian parameters of $Cu^{2+}$ in TGS-family crystals have already been published and are collected in table 1. We used the $g$-factors and hyperfine splitting $A$ for calculations of the d-orbital energies and covalency factors.

The electron spin–lattice relaxation time was determined using the saturation recovery method after saturation with a 24 ns pulse in TGS and a 16 ns pulse in TGFB, having spectral widths of 1.76 and 2.64 mT, respectively, which was sufficient for saturation of the selected hyperfine line. The ESE amplitude was monitored with the Hahn echo produced by two 16 ns pulses with an interpulse interval of 144 ns. The recovery of magnetization after the saturation was single exponential in the whole temperature range (i.e. up to 115 K in TGS) and the relaxation time $T_1$ was obtained by fitting to the equation $M_z(t) = M_0 \exp[1 - \exp(-t/T_1)]$.

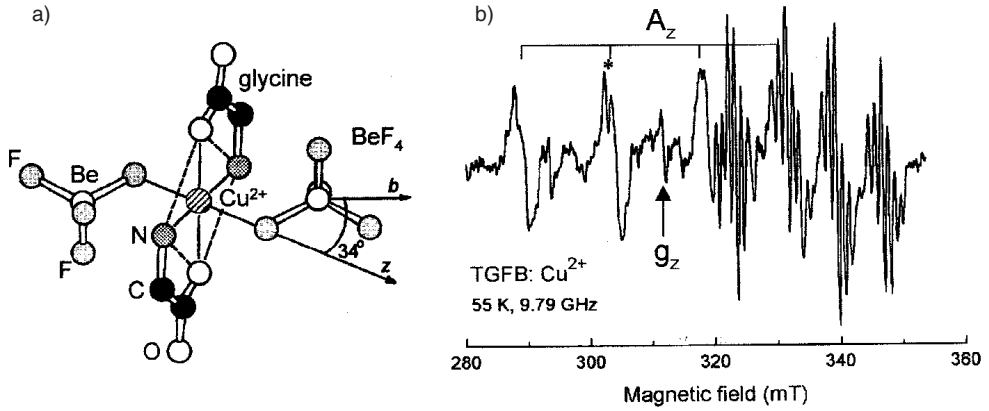


**Figure 1.** (a) Coordination of $Cu^{2+}$ by two glycine ions and two apical $BeF_4$ groups in triglycine fluoroberylate (TGFB) crystal. The $z$-axis of the $g$ and $A$ tensors is marked. (b) EPR spectrum of $Cu^{2+}$ in TGFB recorded at 55 K along the principal $g_z$-axis with hyperfine splitting $A_z$. The spectrum consists of two quartets of hyperfine lines due to two inequivalent $Cu^{2+}$ sites. The asterisk marks the line excited by microwave pulses during ESE experiments.

The temperature range of the pulsed EPR experiments was limited by the amplitude of the ESE signal which becomes practically indetectable at higher temperatures.

## 3. Results and discussion

The spin–lattice relaxation rate $1/T_1$ increases strongly with temperature (figure 2) in a way which is well described by the equation

$$\frac{1}{T_1} = b \cdot T + \frac{9\hbar^2}{\pi^3 \rho^2 v_m^{10}} \left( \frac{\langle s_1 | V^{(1)} | s_2 \rangle}{\Delta_{cr}} \right)^4 \left( \frac{k}{\hbar} \right)^9 T^9 \int_0^{\Theta_D/T} \frac{x^8 e^x}{(e^x - 1)^2} \, dx + f \cdot \mathrm{cosech}^2 \left( \frac{E_{opt}}{2kT} \right) \tag{2}$$

where $v_m^{-10} = (v_L^{-10} + v_{TA}^{-10} + v_{TB}^{-10})/3$ and $v_m$ is the mean sound velocity in a crystal calculated from average values of the longitudinal $v_L$ and transverse $v_{TA}$, $v_{TB}$ wave velocities. The first term describes a small contribution resulting from the non-uniform distribution of $Cu^{2+}$ ions in the crystals as we discussed in [7]. The second term dominates in the relaxation and describes the second-order Raman relaxation process for Kramers ions [8] involving virtual transition via an excited orbital state of energy $\Delta_{cr}$ in a crystal with density $\rho$, sound velocity $v$ (longitudinal $v_L$ and transverse $v_T$). The $\langle s_1 | V^{(1)} | s_2 \rangle$ is the matrix element of spin–phonon coupling (spin–phonon coupling coefficient) between two spin states $s_1$ and $s_2$ with $V^{(1)}$ being the linear term in the expansion of the crystalline electric potential in the power of strain $\varepsilon$ produced by phonons

$$V = V^{(0)} + V^{(1)}\varepsilon + V^{(2)}\varepsilon_1\varepsilon_2 + \cdots. \tag{3}$$

The transport integral $I_8$ (see equation (1)) is given in open form in equation (2) and can be calculated numerically using an algorithm we have already published [9]. The first two terms in equation (2) are sufficient to describe $1/T_1$ for TGSe and TGFB, whereas for TGS crystal, where experimental results were collected up to 115 K, the last term in equation (2) becomes important. This term describes Raman-type relaxation via the local mode [10]. The local mode energy is $E_{opt} = 486\ \mathrm{cm}^{-1}$ in TGS crystal. This energy is higher than the Debye limit, and

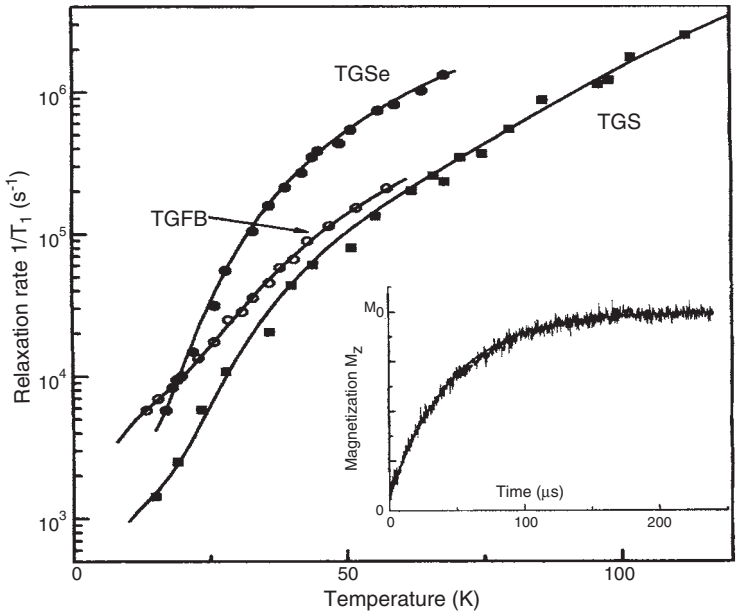


**Figure 2.** Temperature dependence of the spin–lattice relaxation rate. Solid lines are the best fits to equation (2) with parameters collected in table 1. The inset shows recovery of magnetization after pulse saturation at 36 K with $T_1 = 46.7$ $\mu$s.

can thus be identified as an optical phonon mode. Raman spectroscopy data [11] show that this mode is due to optical motions of $SO_4$-groups.

The solid lines in figure 2 are the best fits to equation (2) with parameters and Debye temperatures collected in table 1. The $c$-coefficient is defined as $c \equiv \frac{9\hbar^2}{\pi^3\rho^2 v_m^{10}}\left(\frac{\langle s_1|V^{(1)}|s_2\rangle}{\Delta_{cr}}\right)^4\left(\frac{k}{\hbar}\right)^9$ and its values are collected in table 1.

### *3.1. Debye temperature $\Theta_D$ from elastic constants*

The Debye temperature is related to the cut-off frequency $\omega_D$ of the lattice vibrations in the Debye model $k\Theta_D = \hbar\omega_D$ and is a fitting parameter in equation (2). We have previously determined the Debye temperature for TGSe as $\Theta_D = 168$ K [3]. $\Theta_D$ for TGS was also evaluated from low temperature specific heat measurements, first as 104 K [12] and then corrected to 346.6 K [13]. To confirm one of these values we decided to calculate the Debye temperature from elastic data which are available for TGS [13–15] and TGSe [16] crystals.

The Debye temperature can be calculated as

$$\Theta_D = \frac{\hbar}{k}\sqrt[3]{6\pi^2\frac{N}{V}}v_m = \frac{\hbar}{k}\sqrt[3]{6\pi^2\frac{pN_A\rho}{M}}v_m \tag{4}$$

where $v_m$ is the mean sound velocity in a crystal related to the elastic constants $c_{ij}$, $N/V$ is the number of vibrating units (atoms) in the unit volume, $N_A$ is Avogadro's number, $\rho$ is a crystal density, $p$ is the number of atoms in the molecule and $M$ is the molecular weight of a compound. The equation of motion of a plane wave of amplitude $u_l$ propagating in the crystal along the direction defined by direction cosines $l_i, l_j, l_k$ leads to Christoffel's relation

$$(c_{ijkl}l_j l_k - \rho v^2\delta_{il})u_l = 0 \tag{5}$$

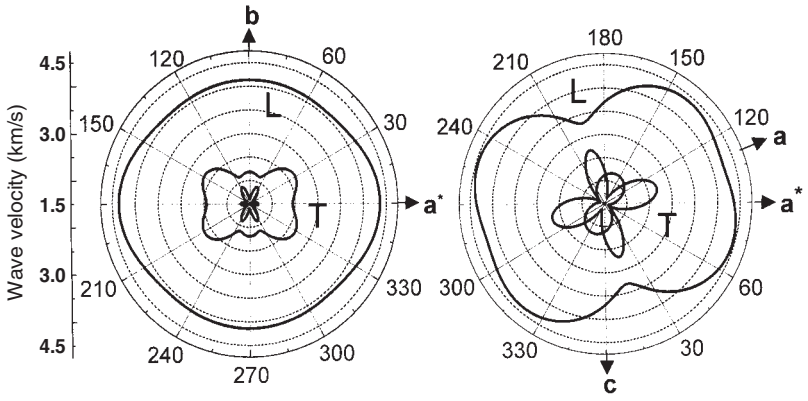


**Figure 3.** Cross section of the wave velocity surface in the $a^*b$ and $ca^*$ plane of TGSe crystal calculated from the elastic constants for longitudinal (L) and two transverse (T) phonons. Note that the velocity coordinate starts from 1.5 km $s^{-1}$.

where $c_{ijkl}$ are elastic tensor components and $\delta_{ij}$ is the Kronecker delta. Equation (5) can be written in a matrix form using $\Gamma_{ij} = \Gamma_{ji} = l_k l_l c_{ikjl}$ and then the three sound velocities are the three roots of the secular equation

$$\begin{vmatrix} \Gamma_{11} - \rho v^2 & \Gamma_{12} & \Gamma_{13} \\ \Gamma_{12} & \Gamma_{22} - \rho v^2 & \Gamma_{23} \\ \Gamma_{13} & \Gamma_{23} & \Gamma_{33} - \rho v^2 \end{vmatrix} = 0. \tag{6}$$

The expanded forms of the $\Gamma_{ij}$ are given in [17, 18] in Cartesian and polar coordinates as a function of the elastic moduli $c_{ij}$ for a given propagation vector $(l_1, l_2, l_3)$. Using 13 elastic moduli for our monoclinic crystals from [13–16] we have calculated the velocity of the longitudinal (L) and two transverse (T) phonons. The velocities are highly anisotropic, as is shown for TGSe crystal in the $a^*b$ and $ca^*$ plane in figure 3.

The average sound velocity was calculated by numerical integration over a solid angle as

$$v_m = \left[ \frac{1}{3} \int_0^{4\pi} \left( \frac{1}{v_L^3} + \frac{1}{v_{TA}^3} + \frac{1}{v_{TB}^3} \right) \frac{d\Omega}{4\pi} \right]^{-1/3} \tag{7}$$

where $d\Omega = \sin\theta \, d\theta \, d\phi$ with a 1° increment in $\theta$ and $\phi$. The average values $v_L$, $v_{TA}$, $v_{TB}$ and $v_m$ are collected in table 2.

Assuming that all 74 atoms in the crystal unit cell of volume $V_u$ (given in table 1) participate in acoustic phonon vibrations we calculated the elastic Debye temperature as 348 K for TGS and 288 K for TGSe. This result for TGS is consistent within the experimental error with the 'corrected' calorimetric Debye temperature 346.6 K.

The Debye temperature for TGFB has been not determined so far. The elastic constants are not available for this crystal either. Thus, keeping in mind the similarity in crystal structure within the TGS family, we have evaluated sound velocities from proportionality $v_m = k_1 \rho^{-1/2}$ and the Debye temperature from $\Theta_D = k_2 \cdot V_u^{-1/3} \rho^{-1/2}$ by calculation of the proportionality coefficients $k_1$ and $k_2$ from $v_m$ and $\Theta_D$ of TGS and TGSe. The results of the evaluation are shown in table 2.

The experimental 'elastic' and 'calorimetric' Debye temperatures are practically identical but are much higher than the $\Theta_D$ determined from the Raman spin relaxation (see table 2). (We found a similar situation in Tutton salt family crystals [7].) All these $\Theta_D$ values are determined from the three different phenomena applying the Debye model of lattice vibration for the interpretation of experimental results.

**Table 2.** Sound velocities, Debye temperature $\Theta_D$ and spin–phonon coupling parameters for $Cu^{2+}$ in TGS-family crystals

| | TGS | TGSe | TGFB |
|---|---|---|---|
| Average sound velocities[a] (m $s^{-1}$) | | | |
| Branches $v_L$, $v_{TA}$, $v_{TB}$ | 4510, 2396, 1969 | 4083, 2133, 1701 | 4757, 2549, 2133 |
| Crystal $v_m$ | 2409 | 2106 | 2590 |
| Debye temperature $\Theta_D$ (K) from | | | |
| Raman relaxation[b] | 190 | 168 | 179 |
| Elastic constants | 348 | 288 | 372 |
| Specific heat [12, 13] | 346.6 | — | — |
| Matrix element of the spin–phonon coupling ($cm^{-1}$)[c] | 553 | 742 | 569 |

[a] Calculated from elastic constants of [14–16].
[b] Error: ±3 K.
[c] Error: ±12 $cm^{-1}$.

The specific heat at a given temperature is a sum of an acoustic phonon contribution and contributions from various thermal excitations. An example of the separation of the various contribution in hexamines is published in paper [19]. Therefore, $\Theta_D$ calculated from $c_v$ is different at different temperatures and it is generally plotted in dependence on the Debye temperature. At low temperatures ($T < \Theta_D/20$) most of the contributions vanish and $c_v$ shows a temperature dependence of approximately $T^3$, well explained by the Debye model. This allows determination of $\Theta_D$ from extrapolation of low-temperature experimental data to the absolute zero temperature [17, 20]. However, the accuracy of the determination of $\Theta_D$ ($T = 0$ K) is limited by the low accuracy of experiments at very low temperatures.

In contrast to the specific heat, the sound velocity in a solid does not seem to have various contributions and depends on the strength of the coupling between atoms and on the interatomic distance. These are weakly temperature dependent due to lattice contraction. As the result, the sound velocity increases at low temperatures, which is usually presented in the form of a temperature dependence of the elastic constants [15, 16]. The increase in $v_m$ on cooling from room temperature to liquid helium temperature is small (lower than 5%) and the calculated $\Theta_D$ from elastic constants at room temperature should be corrected (enlarged) for comparison with the calorimetric value. The accuracy of the $\Theta_D$ determined from sound velocity is limited only by experimental errors in measurements of the elastic constant. However, it should be stressed that at room temperature the real phonon spectra are usually far from the Debye model ($\omega^2$-dependence of the state density), thus the elastic $\Theta_D$ can suffer strongly from this inconsistency.

In the determination of $\Theta_D$ from Raman spin relaxation rather broad low temperature range data are used. In a such temperature range the Debye phonon spectrum with $\omega^2$-dependence is expected to be valid, at least up to about 20 K. Thus, one can expect that the best value of $\Theta_D$ should be obtained from a fit to the low temperature Raman relaxation data. Therefore, the observed discrepancy between the elastic-calorimetric and spin relaxation $\Theta_D$ is strikingly large and needs detailed consideration.

First, one should note that the Raman relaxation term in equation (2), generally used for the fit to experimental data, contains two mutually dependent parameters, i.e. $v_m$ and $\Theta_D$. The relation between these two parameters in terms of the Debye model is given by equation (4). Thus it is reasonable to substitute $v_m$ from equation (4) into (2) to obtain a single variable

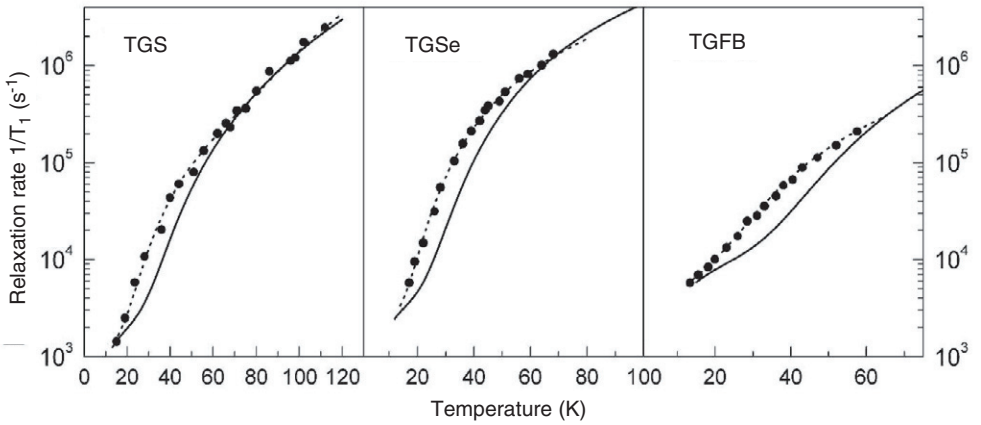


**Figure 4.** Temperature dependence of the spin–lattice relaxation rate with the best fit to equation (2): with resulting $\Theta_D$ temperatures of 190 K for TGS, 168 K for TGSe and 179 K for TGFB as in figure 2 (dashed lines), and with elastic $\Theta_D$ values of 348, 288 and 372 K, respectively (solid lines).

equation which takes a form

$$\frac{1}{T_1}(\text{Raman}) = \frac{9\hbar^3}{k_B}\left(6\pi^{11/10}\frac{pN_A}{M}\rho^{2/5}\right)^{10/3}\left(\frac{\langle s_1|V^{(1)}|s_2\rangle}{\Delta_{cr}}\right)^4\frac{T^9}{\Theta_D^{10}}I_8\left(\frac{\Theta_D}{T}\right)$$
$$= c'\frac{T^9}{\Theta_D^{10}}I_8\left(\frac{\Theta_D}{T}\right). \tag{8}$$

A fit with equation (8) to the experimental data gives the same Debye temperature as a fit to equation (2) with the $c'$-coefficient depending on the molecular parameters of the crystal only. We suggest that a fit with equation (8), instead of equation (2), should be preferred since such a fit is independent of the sound velocity.

One can expect that, in analogy to the specific heat, the low temperature relaxation data could be useful for determination of $\Theta_D$ identical with the calorimetric value. However, the situation is quite the opposite here. Low temperature relaxation can be influenced by, besides the acoustic phonons, many various processes such as tunnelling two-level systems, rotational tunnelling of molecular groups, boson peaks, local vibration modes and cross-relaxation. These contributions, resulting from low energy excitations, are important at low temperatures, whereas at higher temperatures (higher than 100 K) two-phonon Raman processes can dominate. Thus, one should expect a good fit to equations (2) and (8) in the high temperature range but not at low temperatures. To check this we have assumed that the elastic-calorimetric $\Theta_D$ also describes the spin–lattice relaxation and we fit equation (8) to the experimental points using just the $c'$-coefficient as the fitting parameter. The results of fitting are shown by solid lines in figure 4 for TGS, TGSe and TGFB crystals with Debye temperatures of 348, 288 and 372 K, respectively. The dashed lines in figure 4 are the best fits when both $\Theta_D$ and $c'$ were used as the fitting parameters with apparent Debye temperatures of 190 K for TGS, 168 K for TGSe and 179 K for TGFB (as in figure 2). The plots show that there exists a possibility of fitting the temperature dependence of the spin–lattice relaxation rate $1/T_1$ using $\Theta_D$ determined from sound velocity or from specific heat measurements, with a good fit for the high temperature range. But then at low temperatures there should exist an excess of vibrations over the Debye spectrum producing additional contributions to the relaxation. We

are not able to identify these vibrations from our experimental data; this needs further detailed investigations. We suppose that the additional low temperature relaxation processes are related to the dynamics of the doped paramagnetic ions since the ions are local defects disturbing the host lattice, especially since in TGS family crystals the ions are located in interstitial sites.

### *3.2. Orbital splitting and covalency in the Cu(II) complexes*

To draw any additional conclusions from the experimental temperature dependence of the spin–lattice relaxation rate $1/T_1$ and from fits to equations (2) or (8) we have to know the orbital splitting energy $\Delta_{cr}$ and the covalency of the Cu–ligand coordination bonds which can limit the application of crystal field theory to calculation of the electric potential at $Cu^{2+}$ sites. These data can be obtain from analysis of cw-EPR data already published for $Cu^{2+}$ in TGS-family crystals [21–24]. The $g$-factors and hyperfine splitting $A$ for these crystals are collected in table 1. These parameters indicate a $|x^2 - y^2\rangle$ ground state of $Cu^{2+}$ in $D_{2h}$ crystal field symmetry. We have recalculated the results previously published in [21–24] to get consistent values of the resulting parameters.

In $D_{2h}$ symmetry the molecular orbitals of $Cu^{2+}$ can be written as [25]

$$\begin{aligned}
\psi_1(A_g) &= \alpha|x^2 - y^2\rangle - \gamma\Phi_L(A_g)\\
\psi_2(A_g) &= \alpha_1|z^2\rangle - \gamma_1\Phi_L(A_g)\\
\psi_3(B_{1g}) &= \beta_1|xy\rangle - \gamma_2\Phi_L(B_{1g})\\
\psi_4(B_{2g}) &= \beta|xz\rangle - \gamma_3\Phi_L(B_{2g})\\
\psi_5(B_{3g}) &= \beta'|yz\rangle - \gamma_4\Phi_L(B_{3g})
\end{aligned} \tag{9}$$

where $\Phi_L$ are linear combinations of s and p orbitals of the ligands. The spin-Hamiltonian parameters for the antibonding orbitals (9) are [25, 26]

$$\begin{aligned}
g_z &= 2.0023 - 8\alpha^2\beta_1^2\frac{\lambda_0}{E_{xy}}\\
g_y &= 2.0023 - 2\alpha^2\beta^2\frac{\lambda_0}{E_{xz}}\\
g_x &= 2.0023 - 2\alpha^2\beta'^2\frac{\lambda_0}{E_{yz}}
\end{aligned} \tag{10}$$

$$\begin{aligned}
\frac{A_z}{P_0} &= \left(-\kappa - \frac{4}{7}\right)\alpha^2 + \Delta g_z + \frac{3}{14}(\Delta g_y + \Delta g_x)\\
\frac{A_y}{P_0} &= \left(-\kappa + \frac{2}{7}\right)\alpha^2 + \Delta g_y - \frac{3}{14}\Delta g_x\\
\frac{A_x}{P_0} &= \left(-\kappa + \frac{2}{7}\right)\alpha^2 + \Delta g_x - \frac{3}{14}\Delta g_y
\end{aligned} \tag{11}$$

where $\lambda_0$ is the free-ion spin–orbit coupling constant equal to $-829$ cm$^{-1}$, $\kappa$ is the Fermi contact hyperfine constant equal to 0.43 for free $Cu^{2+}$, $P_0 = 0.036$ cm$^{-1}$ describes radial extension of the d-wavefunction of the $Cu^{2+}$ ion, $\Delta g_i = g_i - 2.0023$ and $E_{ij}$ is orbital splitting. For calculation of the molecular orbital (MO) coefficients it is necessary to consider the signs of the $A_i$-parameters, which has been not done previously. $A_z$ has to be negative for $|x^2 - y^2\rangle$ ground state, whereas the signs of $A_y$ and $A_x$ cannot be assumed *a priori*, thus all combinations should be considered. $\alpha^2$ and the Fermi constant $\kappa$ can be calculated from the hyperfine splitting

of equation (11) as

$$\alpha^2 = \frac{7}{12}\left[\frac{A_x + A_y - 2A_z}{P_0} + 2\Delta g_z - \frac{5}{14}(\Delta g_x + \Delta g_y)\right]$$
$$\kappa = \frac{1}{\alpha^2}\left[-\frac{A_z}{P_0} - \frac{4}{7}\alpha^2 + \Delta g_z + \frac{3}{14}(\Delta g_x + \Delta g_y)\right] \tag{12}$$

whereas the $\beta_i$ values can be evaluated from experimental $g$-factors when orbital energies are known from optical spectra. Optical absorption UV–vis spectra of $Cu^{2+}$ in TGS-family crystals are similar to each other and the $|xy\rangle$ orbital energy has been evaluated previously [21–24] (see the first orbital energies in table 1) from the low energy shoulder of the spectra. The energy of other orbitals has not been determined previously from the spectra since the transitions to these states were not resolved. We can evaluate these energies in our calculations. Considering various combinations of the signs of $A_x$ and $A_y$ and discarding unrealistic results (with $\alpha^2 < 0.5$, $\beta^2 < 0.5$ and $\kappa \gg 0.43$) we determine the acceptable sign of hyperfine splitting as shown in table 1. The resulting covalency parameters $\alpha^2$ and $\beta_1^2$ in the ground state are similar in all three crystals and are typical for $Cu^{2+}$ complexes except for TGFB where strong delocalization via $|xy\rangle$ exists. Since any interaction with possible apical ligands ($SO_4^{2-}$, $SeO_4^{2-}$ or $BeF_4^{2-}$) is not noticeable we can assume no delocalization via the $|xz\rangle$ and $|yz\rangle$ orbitals, i.e. $\beta = \beta' = 1$ and appropriate orbital energies can be calculated with the results collected in table 1.

It should be noted that there exist a considerable delocalization of the unpaired electron onto glycine ligands in the main coordination plane both via the ground state $|x^2 - y^2\rangle$ and the excited $|xy\rangle$ state.

### *3.3. Spin–phonon coupling*

Spin–phonon coupling described by the matrix element $\langle s_1|V^{(1)}|s_2\rangle$ in equations (2) and (8) depends on the mechanism of the electron spin–lattice relaxation. For paramagnetic ions this mechanism acts indirectly via spin–orbit interaction which couples spins with fluctuating crystal field potential $V$. This is usually considered by expansion of the crystal field potential in terms of lattice strains produced by the phonons as shown by equation (3).

In second-order two-phonon Raman processes, dominating in the relaxation of Kramers ions, only the second term of the expansion is important. This term describes the dynamical part of ion–lattice interaction with $V^{(1)}$ being an additional electric potential generated by phonons. In theoretical calculations of the spin–phonon coupling it is assumed that $V^{(1)}$ and also higher $V^{(n)}$ are of the same order of magnitude as the static potential $V^{(0)}$ [4]. Thus any of $V^{(n)}$ can be roughly evaluated in terms of the crystal field theory. Such numerical evaluation of the spin–phonon matrix element is known for a few rare-earth salts. For example, in dysprosium ethyl sulfate it was evaluated as $\langle s_1|V^{(1)}|s_2\rangle \approx 10\ \mathrm{cm}^{-1}$ [6]. For the iron-group ions the spin–phonon coupling parameters were considered theoretically using crystal field theory in some ionic solids [27, 28]. These evaluations suffer from use of the point charge approximation typical for the crystal field theory, which seems not be valid in our crystals where considerable covalency of the coordination bond exists, as was shown in the previous section. So, at the current state of our knowledge the spin–phonon coupling parameter $\langle s_1|V^{(1)}|s_2\rangle$ should be considered rather as an unknown parameter in the interpretation of experimental data. A considerable collection of the spin–phonon coupling parameters in various solids can give some indications for the development of a theory for the parameter calculations. In the TGS family we found the spin–phonon coupling parameters from the experimental $c$-coefficient (or $c'$) of the Raman relaxation process (see table 1).The calculated values of $\langle s_1|V^{(1)}|s_2\rangle$ are 553 $\mathrm{cm}^{-1}$ for TGS, 742 $\mathrm{cm}^{-1}$ for TGSe and 569 $\mathrm{cm}^{-1}$ for TGFB. These values of $\langle s_1|V^{(1)}|s_2\rangle$ are about two orders of magnitude

higher than those for rare-earth ions, reflecting the higher crystal field potential acting on the 3d-electrons. The difference between the coupling in TGS-family crystals displays a sensitivity of the coupling to the details of the electronic structure and dynamics of $Cu(gly)_2X_2$ complexes in the host lattices.

## 4. Conclusions

The Debye temperature $\Theta_D$ is still widely used as a single parameter characterizing thermal crystal lattice vibrations. Classical methods for determining $\Theta_D$, i.e. specific heat at very low temperatures and elastic constant measurements, give mutually consistent values of $\Theta_D$ when properly interpreted. Electron spin–lattice relaxation measurements can be described assuming the Raman relaxation processes involving a whole Debye-type phonon spectrum. However, the resulting $\Theta_D$ is usually much higher than the calorimetric and elastic Debye temperature. We show that it is necessary to assume that as well as the Raman relaxation processes another relaxation process operates and is related to the low-lying local excitations. Then, the $\Theta_D$ obtained from other methods can be used for description of experimental relaxation data and for calculation of the effective electron–phonon coupling parameter.

## References


[1] Jona F and Shirane G 1962 *Ferroelectric Crystals* (Oxford: Pergamon)
[2] Stankowski J 1981 *Phys. Rep.* **77** 1
[3] Hoffmann S K, Hilczer W and Goslar J 1996 *J. Magn. Reson.* A **122** 37
[4] Orbach R and Stapleton H J 1972 *Electron Paramagnetic Resonance* ed S Geschwind (New York: Plenum) chapter 2
[5] Orbach R 1961 *Proc. R. Soc.* A **264** 458
[6] Blume M and Orbach R 1962 *Phys. Rev.* **127** 1587
[7] Hoffmann S K, Hilczer W, Goslar J and Augustyniak-Jablokow M A 2001 *J. Phys.: Condens. Matter* **13** 7443
[8] Abragam A and Bleaney B 1970 *Electron Paramagnetic Resonance of Transition Ions* (Oxford: Clarendon) chapter 10
[9] Hoffmann S K, Hilczer W, Goslar J, Massa M M and Calvo R 2001 *J. Magn. Reson.* **153** 92
[10] Goslar J, Hoffmann S K and Hilczer W 2002 *Solid State Commun.* **121** 423
[11] Winterfeldt V, Schaack S and Klöpperpieper A 1977 *Ferroelectrics* **15** 21
[12] Lawless W N 1976 *Phys. Rev.* B **14** 134
[13] Lawless W N 1978 *Phys. Rev.* B **17** 1458
[14] Haussühl S and Albers J 1977 *Ferroelectrics* **15** 73
[15] Minayeva K A, Baryshnikova E V, Strukov B A and Varikash W M 1978 *Kristallografija* **23** 646 (in Russian)
[16] Luspin Y and Hauret G 1977 *Ferroelectrics* **15** 43
[17] Alers G A 1965 *Physical Acoustics* ed W P Mason (New York: Academic) chapter 1
[18] Robie R A and Edwards J L 1966 *J. Appl. Phys.* **37** 2659
[19] Piekara-Sady L and Stankowski J 1988 *Physica* B **152** 347
[20] Huffman D R and Norwood M H 1960 *Phys. Rev.* **117** 709
[21] Stankowski J 1967 *Phys. Status Solidi* **24** 451
[22] Stankowski J, Wieckowski A and Hedewy S 1974 *J. Magn. Reson.* **15** 498
[23] Goslar J, Szczepaniak L and Dezor A 1983 *Acta Phys. Pol.* A **63** 671
[24] Hoffmann S K and Makowska B 1979 *Acta Phys. Pol.* A **56** 527
[25] McGarvey B R 1966 *Transition Metal Chemistry* vol 3, ed R L Carlin (New York: Dekker)
[26] Attanasio D 1977 *J. Magn. Reson.* **26** 81
[27] van Vleck J H 1940 *Phys. Rev.* **57** 426
[28] Altshuler S A and Kozyrev B M 1972 *Electron Paramagnetic Resonance of Transition Ion Compounds* (Moscow: Nauka) chapter 5 (in Russian)
[29] Hoshino S, Okaya Y and Pepinsky R 1959 *Phys. Rev.* **115** 323
[30] Kay M I and Kleinberg R 1973 *Ferroelectrics* **5** 45
[31] Zheludev I S 1968 *Physics of Crystalline Dielectrics* (Moscow: Nauka) (in Russian)